Available online at www.sciencedirect.com
ScienceDirect
Journal of Molecular Catalysis A: Chemical 268 (2007) 257–263
JOURNAL OF MOLECULAR CATALYSIS A: CHEMICAL
www.elsevier.com/locate/molcata

Dopant influence on the photo-catalytic activity of TiO_2 films prepared by micro-plasma oxidation method

Wu Xiaohong *, Qin Wei, Ding Xianbo, He Weidong, Jiang Zhaohua

Harbin Institute of Technology, Harbin 150001, PR China

Received 2 September 2006; received in revised form 10 December 2006; accepted 11 December 2006
Available online 19 December 2006

Abstract

Mesoporous titanium dioxide films were fabricated on titanium plates by the micro-plasma oxidation method. To increase the photo-catalytic activity of the films, $Eu(NO_3)_3$ of different concentrations were added to the H_2SO_4 electrolyte solution. Eu incorporation was found in the porous titania films. Furthermore, Na_2SiO_3 of different concentrations was also added to the electrolyte solution, which led to Si incorporation into the film as well. A model textile industry pollutant (Rhodamine B) was used to study the photo-catalytic properties of the modified films. The photo-catalytic activity of these films turned out to be improved by the additives to the electrolyte solution. The enhanced photo-catalytic activity might result from (i) the increased porosity, producing more reactive sites to absorb and oxide pollutants; (ii) electron trapping at Eu sites suppressing the e^-/h^+ pair recombination, therefore, improving the photo-catalytic processes.

Keywords: Micro-plasma oxidation; Ions doping; Titanium dioxide; Photocatalysis

1. Introduction

Titania is one of the most studied semiconductors for photo-catalytic reactions due to its low cost, ease of handling and high resistance to photo-induced decomposition [1,2]. In recent years, many studies have been focused on the use of titanium dioxides (TiO_2) in applications such as gas sensors [3], waveguides [4], solar energy cells [5] and photo-catalysts [6]. Among these various applications of TiO_2, the photo-catalytic effects have been paid much more attention to in the fields of purification and treatment of polluted water and air. Although colloidal and particulate TiO_2 catalyst suspensions have high photo-degradation efficiency for organic compounds, separation of the catalysts from the system after the reaction is difficult. Therefore, particles are not very amenable to reuse of the catalyst.

In order to improve photo-catalytic efficiency, tremendous efforts have been made in recent years, which include the synthesis of composite photo-catalysts [7–10] and the change of the TiO_2 film character. TiO_2 doped by certain types of transition metals has been extensively studied since these transition metal clusters could elongate electron–hole pair separation [11,12]. TiO_2 films have been prepared by a variety of deposition techniques such as the sol–gel process, chemical vapor deposition, etc. [13–17]. But these approaches are complicated, expensive or not environmental friendly. Besides, coatings produced by these methods present a weak adherence to substrates and are not uniform. However, a new coating technology, micro-plasma oxidation (MPO) was developed [18]. This method is based on the anodic oxidation, which occurs at potentials above the breakdown voltage of the oxide film growing on the anode surface [19]. In certain electrolyte solutions, MPO occurs only in a high cell voltage. The process consists of numerous simultaneous and uniform plasma discharges over the metal surface. Uniform films are synthesized in the plasma discharge process and the films have good adherence to substrates. And the instantaneous temperature of the films can exceed 2000 °C in this method, which makes it easy for dopant to be added in titania films [20].

Considering that the dopant of Eu ions can improve the photo-catalytic activity of the thin TiO_2 films [21] and SiO_3^{2-} ions can help the films grow, MPO was used to prepare TiO_2 films on titanium substrates in this paper. Eu ions of different concentrations were added to the H_2SO_4 electrolyte solution in the process of MPO. And then Na_2SiO_3 of different concentrations were added

* Corresponding author. Present address: Department of Applied Chemistry, Harbin Institute of Technology, Harbin 150001, PR China.
Tel.: +86 451 8640 2522; fax: +86 451 8640 2522.
E-mail address: wxhqw@263.net (W. Xiaohong).

1381-1169/$ – see front matter © 2006 Elsevier B.V. All rights reserved.
doi:10.1016/j.molcata.2006.12.022

to the H_2SO_4 and $Eu(NO_3)_3$ electrolyte solution. Rhodamine B as model compound was used to test the photo oxidation efficiency of the films under ultraviolet (UV) irradiation (365 nm). The objective of this research was to investigate the effects of Na_2SiO_3 and $Eu(NO_3)_3$ of different concentrations on the surface morphology, structural properties and the photo-catalytic activity of the modified films.

2. Experimental

2.1. Preparation and characterization of TiO_2 films

A titanium sheet (99.9% in purity) was selected as anode, with a reaction area of 25 mm × 10 mm × 0.5 mm and a copper sheet was introduced as cathode. The set-up scheme is shown in Fig. 1. The anode was located in the center of the electrolyte cell. The MPO process with a homemade 3 kW dc power supply was conducted in two stages: the galvanostatic anodization with a constant current density was first performed until a designated anode-to-cathode voltage was reached, and then the voltage was maintained until the end of oxidation, with a gradual decrease in the current. The temperature was controlled in the range (20 ± 0.2 °C) by a cold water jacket. The electrolyte solution I consisted of 0.5 M analytical-grade H_2SO_4 and different concentrations of analytical-grade $Eu(NO_3)_3$. The electrolyte solution II consisted of 0.5 M analytical-grade H_2SO_4, 0.04 g/L analytical-grade $Eu(NO_3)_3$ and different concentrations of analytical-grade Na_2SiO_3 solutions. All the aqueous solutions were prepared with distilled water. The produced films were then rinsed in distilled water and dried in a current of hot air. The films generated by this method were marked as TiO_2, TiO_2 + Eu, TiO_2 + Eu + Si, respectively. According to the previous work [22], thin TiO_2 films had higher photo-catalytic activity when the current density was 80 mA/cm^2, the voltage was 160 V and the oxidation time was 10 min. The above process parameters kept constant in this research.

2.2. Characterization of TiO_2 films

Scanning electronic microscopy (SEM) (D/max-rB) was used to study the surface morphology and pore distribution of the produced films. Surface morphology, roughness and the maximum height of projection of the modified TiO_2 films were examined with a digital Instruments Nanoscope III atomic force microscope (AFM), operating in the tapping mode (TM).

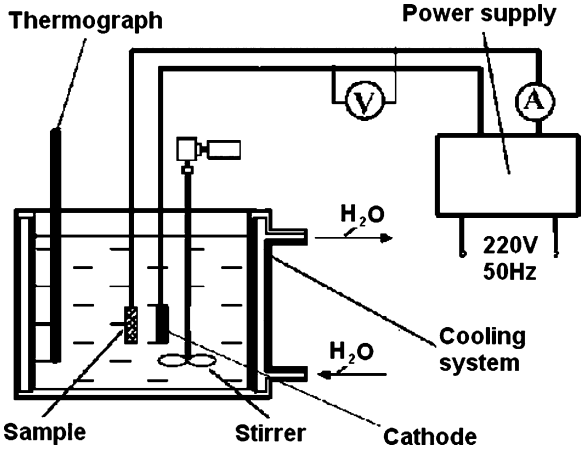

Fig. 1. Schematic view of the micro-plasma oxidation set-up.

The crystalline structure of the films was examined by X-ray diffraction (XRD) with the Cu Kα source. The accelerating voltage and applied current were 40 kV and 30 mA, respectively. The compositions of TiO_2 films were analyzed through X-ray photoelectron spectroscopy (XPS) with the Al Kα source generated by a VG Scientific ESCALAB Mark II spectrometer, equipped with two ultrahigh-vacuum (UHV) chambers. The pressure in the chamber during the experiments was approximately 2.4×10^{-6} Pa. X-ray photoelectron spectra were referenced to the C 1s peak ($E_b = 284.6$ eV) resulting from the adventitious hydrocarbon (i.e. from the XPS instrument itself) present on the surfaces of the films.

2.3. Photo-catalytic measurement

The bench-scale photoreactor system consisted of a cylindrical quartz cell with the size of 25 mm in diameter and 50 mm in height and a 20 W UV lamp with a maximum UV-irradiation peak of 365 nm. The schematic diagram of photoreactor was presented in a previous paper [23]. The photo-catalytic activity of each films produced by MPO was examined by measuring the degradation of the Rhodamine B dye solution. Films of 2.5 cm^2 were immersed into the 10 mL aqueous Rhodamine B solution (10 mg/L). The solution was stirred continuously and supplied with air in the reaction process. The UV light was irradiated for 2 h perpendicularly to the surface of the samples through the sidewall of the cylindrical quartz cell. The distance between the UV source and the films was 2 cm. Rhodamine B had the maximum absorbance at the wavelength of 552 nm in the UV spectrometry. The change of Rhodamine B concentration with the irradiation time was measured by UV spectrophotometry at the wavelength of 552 nm.

3. Results

3.1. Photo oxidation efficiency of TiO_2 films

Firstly, the pollutant solution was photolyzed in the absence of the photocatalyst to examine its stability. The experiments under UV-illumination demonstrate that the removal speed of Rhodamine B is very low in the absence of TiO_2 films. The degradation efficiency of Rhodamine B using the produced films (TiO_2, TiO_2 + Eu) and that in the absence of the films are shown in Fig. 2. It can be seen that the doped films enhance the efficiency of degradation and the speed of photocatalytic degradation increases gradually with the $Eu(NO_3)_3$ concentration of. When the dopant concentration is 0.04 g/L, the photo-degradation efficiency is the best. The removal of Rhodamine B using the films with UV-irradiation of 15 min reaches 62%, which is 24% higher than that using the films produced in the pure H_2SO_4 electrolyte solution.

Based on this research, TiO_2 + Eu + Si films were prepared with the electrolyte solution II. The degradation of Rhodamine B

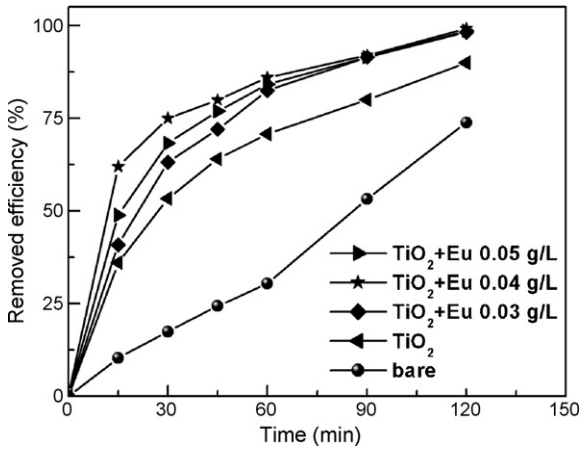

Fig. 2. Photo-catalytic degradation of Rhodamine B by TiO_2 thin films produced at different condition.

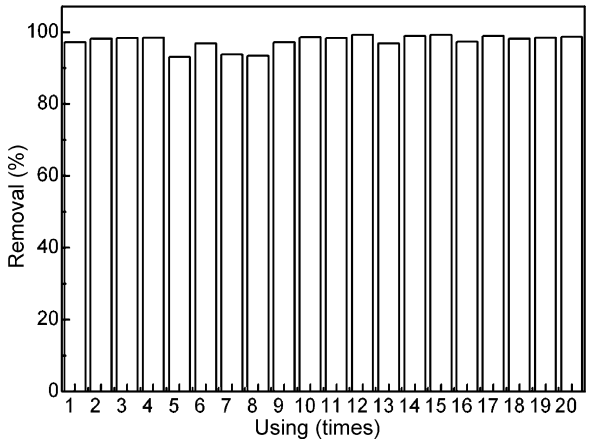

Fig. 4. Reuse of films prepared with micro-plasma oxidation method.

using the produced films (TiO_2 + Eu, TiO_2 + Eu + Si) is shown in Fig. 3. It can be seen that the speed of Rhodamine B degradation reaches the maximum when the concentration of the Na_2SiO_3 is 0.5 g/L. The removal of Rhodamine B using the films with UV-irradiation of 15 min reaches 81.5%, which is 19.5% higher than that using the films produced with the electrolyte solution in the absence of Na_2SiO_3.

TiO_2 + Eu + Si films were used repeatedly as many as 20 times. The degradation of Rhodamine B for 120 min is shown in Fig. 4. It can be seen that the removal efficiencies of Rhodamine B all exceed 98%.

3.2. Surface morphology of the films

Characteristic SEM photographs of three films (TiO_2, TiO_2 + Eu, TiO_2 + Eu + Si) magnified by 3000 times are presented in Fig. 5. It can be seen that the surface of micro-plasma oxidation films are mesoporous. Compared with pure TiO_2, the surface grain size and the density of the pores on TiO_2 + Eu and TiO_2 + Eu + Si films increase, and furthermore TiO_2 + Eu + Si films own a larger extent of increase than TiO_2 + Eu films.

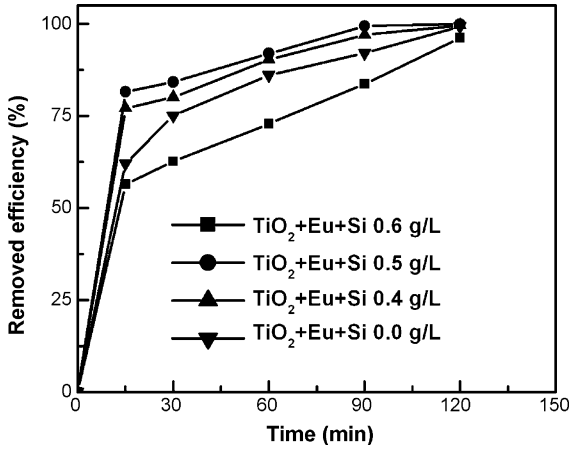

Fig. 3. Photo-catalytic degradation of Rhodamine B by TiO_2 thin films produced at different condition.

In parallel to the SEM photographs, AFM images for the above three samples are shown in Fig. 5. These images show comparable results to the SEM ones verifying the better uniformity for the TiO_2 + Eu and TiO_2 + Eu + Si films. The value of the mean roughness can be obtained directly from these AFM images. The roughnesses of TiO_2, TiO_2 + Eu, TiO_2 + Eu + Si films were 42.893, 81.503, 86.865 nm, respectively. The above results indicate that the roughness of the films increased when $Eu(NO_3)_3$ and Na_2SiO_3 were added to the electrolyte solution.

3.3. Structural analysis of the films

The films prepared under different conditions were examined by XRD. The XRD spectra are shown in Fig. 6, in which the peaks of the substrate Ti, the anatase and rutile forms of TiO_2 are labeled as T, A, and R, respectively.

From Fig. 6A, it can be noticed that the produced films consist of much anatase phase and less rutile phase, and no new crystal phases are produced by doping. Fig. 5b displays the enlarged XRD peaks of anatase TiO_2 planes A(1 0 1) in the 2θ region of 24.0–26.0°. It can be found from Fig. 6B that the X-ray diffraction peaks of crystal plane A(1 0 1) shift to a smaller diffraction angle when $Eu(NO_3)_3$ is added. And this change continues when Na_2SiO_3 is added to the electrolyte solution. The diffraction angle is minimized when the concentration of the Na_2SiO_3 is 0.5 g/L. The X-ray diffraction peaks of crystal plane (1 0 1) and (2 0 0) in anatase are selected to determine the lattice parameters of the produced TiO_2 films. The calculated results of the doped film parameters are shown in Table 1. It can be seen from this table that the cell volume and lattice parameters (a, b and c) increase with doping, and the increase reaches the maximum when 0.04 g/L $Eu(NO_3)_3$ and 0.5 g/L Na_2SiO_3 were doped.

This table also indicates that the content of the anatase TiO_2 increases with the Na_2SiO_3 concentration. When the concentration of Na_2SiO_3 is 0.5 g/L, the TiO_2 ratio of anatase to rutile reaches 80%.

The chemical composition of the TiO_2, TiO_2 + Eu (0.04 g/L), TiO_2 + Eu + Si (0.5 g/L) films was determined by XPS. Typical

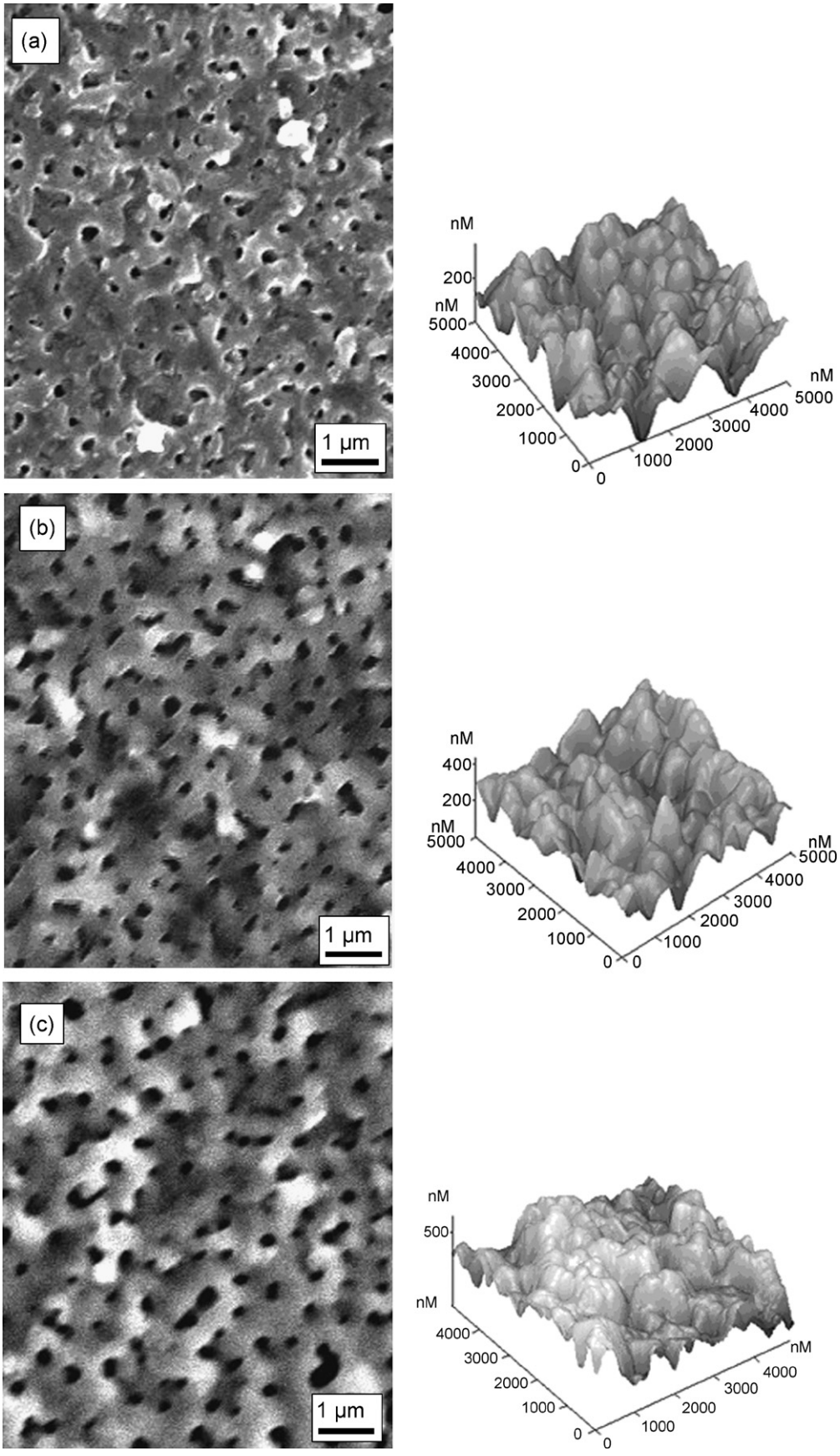

Fig. 5. SEM (left) and AFM (right) images under different conditions: (a) TiO_2; (b) TiO_2 + Eu; (c) TiO_2 + Eu + Si.

Table 1
Effect of additive dopant concentration on lattice parameter of anatase TiO_2

	TiO_2	TiO_2 + Eu	TiO_2 + Eu + Si 0.4 g/L	TiO_2 + Eu + Si 0.5 g/L	TiO_2 + Eu + Si 0.6 g/L
$a = b$, c (nm)	$a = 0.3783$, $c = 0.9499$	0.3791, 0.9531	0.3807, 0.9556	0.3796, 0.9840	0.3785, 0.9522
Cell volume (nm^3)	0.1359	0.1370	0.1385	0.1418	0.1372
Composition (%)	70	70	74	80	75
k_{app} (min^{-1})	0.01765	0.03442	0.03874	0.05301	0.02276

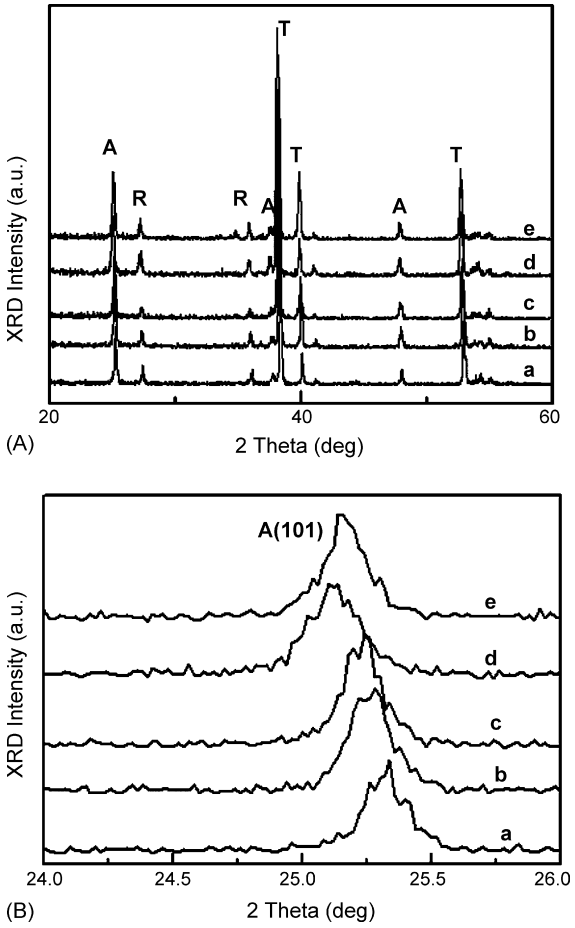

Fig. 6. XRD patterns under different conditions—(A) absolute patterns; (B) partial patterns: (a) TiO_2; (b) TiO_2 + Eu; (c) TiO_2 + Eu + Si 0.4 g/L; (d) TiO_2 + Eu + Si 0.5 g/L; (e) TiO_2 + Eu + Si 0.6 g/L.

survey spectra are presented in Fig. 7. It can be seen that the peaks mainly contain Ti 2p, O 1s, C 1s and O kvv. The peaks of the Eu 4d (1105.94 eV) appear in the survey spectra of the TiO_2 + Eu and TiO_2 + Eu + Si films. Also Si 2p (102.27 eV) appears in the survey spectra of the TiO_2 + Eu + Si films, which implies that Eu^{3+} ions have entered TiO_2 + Eu and TiO_2 + Eu + Si films and that Si^{4+} ions have entered TiO_2 + Eu + Si films. However, the intensity of the Eu 4d and Si 2p peaks are weak, which indicates that the amount of these two kinds of ions in the films is small, so it cannot be detected by XRD.

4. Discussion

Firstly, from the photo-catalytic experiments, SEM photographs and XRD spectra, it can be seen that TiO_2 crystallite and pores are formed on the surface of the Ti substrate and this kind of films have photo-catalytic properties. From the reuse experiment of TiO_2 (Fig. 4), after 20 times of reuse, the films have no changes and the removal efficiency of Rhodamine B is still above 98% for 120 min, which indicates that the films have good adherence to substrates and good photo-catalytic stability. And from the XPS survey spectra, the dopant has entered films by the MPO method. And the dopant has influence on photo-catalytic activity.

The kinetic linear simulation curve of photo-catalytic degradation Rhodamine B upon pure TiO_2 films is shown in Fig. 8. Detailed analysis of the photocatalysis kinetics proves that the Rhodamine B concentration decreases with illumination, which fits well with the first-order exponential decay curve. So it follows the first-order reaction kinetics. It has been well established [24] that photocatalysis experiments follow the Langmuir–Hinshelwood model, where the reaction rate R is

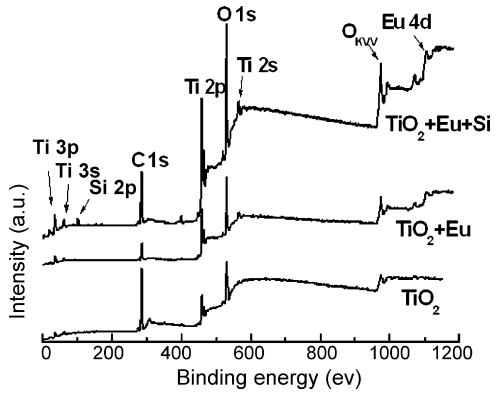

Fig. 7. XPS spectroscopy of TiO_2, TiO_2 + Eu and TiO_2 + Eu + Si films.

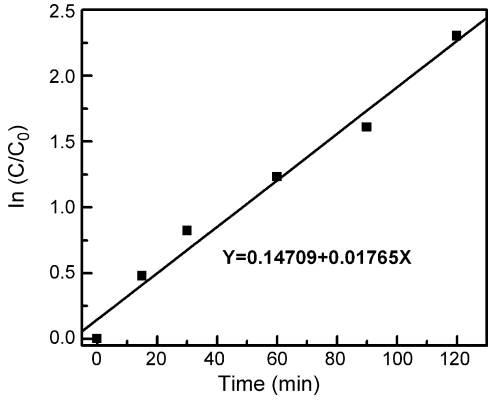

Fig. 8. Relationship between $\ln(C/C_0)$ and reaction time using pure TiO_2 film.

proportional to the surface coverage θ (Eq. (1)):

$$R = -\frac{dC}{dt} = k_r\theta = \frac{k_r KC}{1 + KC} \quad (1)$$

where k_r is the reaction rate constant, K the adsorption coefficient of the reactant at the surface of the film and C is its concentration. When C is very small, the KC product is negligible with respect to unity so that Eq. (1) describes first-order kinetics. The integration of Eq. (1) with the limit condition that at the start of irradiation, $t = 0$, the concentration is the initial one, $C = C_0$, gives

$$-\ln\frac{C}{C_0} = k_{app}\theta = k_r Kt \quad (2)$$

where k_{app} is the apparent first-order reaction constant. The values of k_{app} for the various samples deduced from the graphs of Figs. 2 and 3 and Eq. (2) are given in Table 1. It can be seen that k_{app} value increase with the dopant concentration, and the k_{app} value reaches its maximal when the concentration of Na_2SiO_3 is 0.5 g/L. Changes in the k_{app} value are attributed, via Eq. (2), corresponding to variations in the K value, i.e. different reactant absorption amounts in the surface of the films or equivalent to different surface coverages (θ).

As is known, there are many factors that affect the photo-catalytic activity of TiO_2 films, such as crystalline structure, specific surface area and porosity [25].

From SEM photographs, the surface grain size and the density of the pores increase with the Eu^{3+} and Si^{4+} added in films. This change could improve the photo-catalytic activity of the films because more mesopores can produce more reactive sites to absorb and oxide pollutants. AFM images show comparable results to the SEM ones verifying the better uniformity for the TiO_2 + Eu and TiO_2 + Eu + Si films, and the mean roughness of the films also increases with doping. The above results enable the film surfaces to better absorb and decompose organic compounds. TiO_2 + Eu + Si films express more changes than TiO_2 + Eu films.

From XRD results, it can be seen that the cell volume and lattice parameters (a, b and c) increase and more defects formed with doping. Sclafani and Herrmann have found that metal oxides with more structure defects on surface could ionosorb oxygen as O^- species, which can cause hole trap reaction and produce more $OH^\bullet$ [26]. So, the above lattice defects can reduce the recombination rate of e^-/h^+ pairs and produce more $OH^\bullet$, which has a positive influence on the photo-catalytic activity of the films. When Na_2SiO_3 (0.075 g/L) and $Eu(NO_3)_3$ (0.04 g/L) are added, the lattice distortion of TiO_2 is the maximal. Therefore, the film has higher photo-catalytic activity, which is consistent with the results of the photo-catalytic degradation experiments. The change of phase composition shown in Table 1 is mainly due to the Si ions increasing the amount of the anatase TiO_2 in the MPO process, which also have a positive effect on the enhanced photo-catalytic activity.

The presence of the Eu^{3+} ions on the surface of the films may promote the following reactions (3) and (4) [21]:

$$e^- + Eu^{3+} \rightarrow Eu^{2+} \quad (3)$$

$$O_2 + Eu^{2+} \rightarrow O_2^- + Eu^{3+} \quad (4)$$

Thus, the increase of the photo-catalytic efficiency with the increase of the Eu^{3+} ion concentration may be attributed to the electrons trapped in Eu sites, which are subsequently transferred to absorbed O_2. When the concentration of $Eu(NO_3)_3$ is lower than 0.04 g/L, the degradation efficiency increases gradually with the concentration of $Eu(NO_3)_3$. However, the photoreactivity of the catalyst decreases abruptly when the concentration of $Eu(NO_3)_3$ reaches 0.05 g/L. This means that heavy doping may make the dopants become the recombination centers of the photoexcited electrons, thus reduce the photo-catalytic efficiency.

The XRD and XPS spectra indicate that the bond of Ti–O–Eu might be formed by doping of Eu^{3+} ions. This bond can enhance the surface acidity of TiO_2 films. The higher acidity helped surface to absorb more hydroxyl groups, which could accept more photoexcitated holes and produce more strong surface free radicals to oxidate adsorbed molecules. The spectra also indicate that Ti–O–Si might be formed, which increase in the photo-catalytic activity of the TiO_2 films. An interface of this type has been described for systems containing TiO_2 and SiO_2 and has been shown to possess sites of high Bronsted acidity [27]. Films possessing regions of mixed Ti–O–Si have been shown to increase the removal rate of Rhodamine B by peroxide in aqueous solutions relative to one component TiO_2 or SiO_2 catalysts [27]. So, the increased activity in the films of this paper is also attributed to the phase of Ti–O–Si.

5. Conclusion

In conclusion, TiO_2 films were produced by the micro-plasma oxidation method in the H_2SO_4 electrolyte solution. When Eu^{3+} and Si^{4+} ions were added, the films exhibited higher photo-catalytic activity. The removal of Rhodamine B reached 62% in the initial 15 min, which was 24% higher than that using the films produced in pure electrolyte solution when $Eu(NO_3)_3$ concentration was 0.04 g/L. When Eu^{3+} and Si^{4+} ions were added, the removal of Rhodamine B reached 81.5% in the initial 15 min, which was 19.5% higher than that using TiO_2 + Eu films when the concentrations of Na_2SiO_3 and $Eu(NO_3)_3$ were 0.5 and 0.04 g/L, respectively. The enhanced activity was related to the changes of the lattice parameters, surface structure and composition induced by doping.

Acknowledgments

The authors would like to thank their co-workers for many useful and helpful discussions. Financial support from the Spaceflight Science and Technology Innovation Fund (Project No. HTCXJJ05HIT11) is gratefully acknowledged.

References

[1] A. Fujishima, K. Hashimoto, T. Watanabe, Fundamentals and Applications, BKC, Inc., Tokyo, 1999.
[2] H. Hayashi, K. Torii, J. Mater. Chem. 12 (2002) 3671.
[3] I. Hayakawa, Y. Iwamoto, K. Kikuta, S. Hirano, Sens. Actuators B 62 (2000) 55.

[4] A. Bahtat, M. Bouazaoui, M. Bahatat, C. Garapon, B. Jacquier, J. Mugnier, J. Non-Cryst. Solids 202 (1996) 16.
[5] U. Bach, D. Lupo, P. Comte, J.E. Moser, F. Weissortel, J. Salbeck, H. Spreitzer, M. Gratzel, Nature 395 (1998) 583.
[6] C.A. Linkous, G.J. Carter, D.B. Locuson, A.J. Ouellette, Environ. Sci. Technol. 34 (2000) 3796.
[7] S. Ito, T. Deguchi, K. Imai, H. Tada, Electrochem. Solid-State Lett. 2 (1999) 440.
[8] N.R. Tacconi, C.A. Boyles, K. Rajeshwar, Langmuir 16 (2000) 5665.
[9] H. Nur, S. Ikeda, B. Ohtani, Chem. Commun. (2000) 2235.
[10] S.W. Lee, W.M. Sigmund, Chem. Commun. (2003) 780.
[11] H. Gerishe, J. Phys. Chem. 88 (1984) 6069.
[12] B. Ohtani, R.M. Bowman, D.P. Colombo, H. Kominami, H. Noguchi, K. Uosaki, Chem. Lett. 27 (1998) 579.
[13] J. Sabate, M.A. Anderson, H. Kikkawa, Q. Xu, S. CerveraMarch, C.G. Hill, J. Catal. 134 (1992) 36.
[14] G.A. Battiston, R. Gerbasi, M. Porchia, A. Marigo, Thin Solid Films 239 (1994) 186.
[15] L.M. Williams, D.W. Hess, J. Vasc. Sci. Technol. A 1 (1983) 1810.
[16] T. Fujii, N. Sakata, J. Takada, Y. Miura, Y. Daitoh, M. Takamo, J. Mater. Res. 9 (1994) 1468.
[17] H. Tang, K. Prasad, R. Sanjines, P.E. Schmid, F. Levy, J. Appl. Phys. 75 (1994) 2042.
[18] A.L. Yerokhin, A.A. Voevodin, V.V. Lyubimov, J. Zabinski, M. Donley, Surf. Coat. Technol. 110 (1998) 140.
[19] S. Ikonopisov, Electrochim. Acta 22 (1977) 107.
[20] S.V. Gnedenkov, O.A. Khrisanfova, A.G. Zavidnaya, S.L. Sinebrukhov, A.N. Kovryanov, T.M. Scorobogatova, P.S. Gordienko, Surf. Coat. Technol. 123 (2000) 24.
[21] P. Yang, C. Lu, N. Hua, Mater. Lett. 57 (2002) 794.
[22] X. Wu, Z. Jang, H. Liu, X. Li, X. Hu, Mater. Chem. Phys. 80 (2003) 39.
[23] X. Wu, Z. Jang, H. Liu, S. Xin, X. Hu, Thin Solid Films 441 (2003) 130.
[24] H. Al-Ekabi, N. Serpone, J. Phys. Chem. 92 (1988) 5726.
[25] S.K. Zheng, T.M. Wang, G. Xiang, C. Wang, Vacuum 62 (2001) 361.
[26] A. Sclafami, J.M. Herrmann, J. Phys. Chem. 100 (1996) 13655.
[27] C. Anderson, A.J. Bard, J. Phys. Chem. B 101 (1997) 2611.